TRENDS IN SCIENCES 2026; 23(4): 11608
https://doi.org/10.48048/tis.2026.11608 RESEARCH ARTICLE

Potential of Neolignan from *Piper Crocatum* as Antimicrobial Against Pathogenic Oral Microbes and its Prospects as an Oral Medication

Leny Heliawati[1,*], Seftiana Lestari[2], Yusrina Imani[2], Tri Aminingsih[1], Asri Wulandari[1] and Dikdik Kurnia[2]

[1]*Department of Chemistry, Faculty of Mathematics and Natural Sciences, Universitas Pakuan, Bogor 16129, West Java, Indonesia*
[2]*Department of Chemistry, Faculty of Mathematics and Natural Sciences, Universitas Padjadjaran, Sumedang 45363, West Java, Indonesia*

([*]Corresponding author's e-mail: leny_heliawati@unpak.ac.id)

Received: 15 August 2025, Revised: 3 September 2025, Accepted: 13 September 2025, Published: 30 December 2025

Abstract

Red Betel (*Piper crocatum*) is one of the potential medicinal plants in several traditional medicines, one of which is in the treatment of microbial dental and oral infections. This activity comes from the presence of active secondary metabolite compounds such as neolignan groups which have unique and diverse structures and activities. The aim of this study was to isolate antimicrobial active compounds from red betel leaves and predict their inhibitory mechanism against DNA ligase and lanosterol 14α demethylase enzymes. This study was conducted by isolating red betel leaf extract using column chromatography method in a bioassay guided. The compounds obtained were analysed using UV-Vis, IR, NMR, MS and their antimicrobial activity was tested *in vitro* and *in silico* against *S. mutans*, *S. sanguinis*, *E. faecalis* bacteria, and *C. albicans* fungi. Two compounds were successfully isolated from *P. crocatum* leaves, namely crocatin B (1) and crocatin A (2). crocatin B (1) was found to be capable of inhibiting the growth of *S. mutans* ATCC 25175, *S. sanguinis* ATCC 10556 and *E. faecalis* ATCC 29212. crocatin A demonstrated inhibitory activity against *S. sanguinis*. The binding affinity of crocatin B (1) and crocatin A (2) to the DNA ligase enzyme was –6.14 and –7.27 kcal/mol, respectively, while the binding affinity of crocatin B (1) and crocatin A (2) to lanosterol 14α demethylase was –7.91 and –9.04 kcal/mol, respectively. It is evident from the analysis of pharmacokinetic (ADMET) parameters that both crocatin B (1) and crocatin A (2) demonstrate a satisfactory alignment with the predicted pharmacokinetic parameters. In the context of drug likeness analysis, crocatin B and crocatin A do not demonstrate any violation of the established parameters and are thus classified within the toxicity class 4 category. The data demonstrate the potential of crocatin B (1) and crocatin A (2) as antimicrobials against oral pathogenic microbes, as evidenced by *in vitro* and *in silico* studies.

Keywords: Red betel (*Piper crocatum*), Neolignan, Antimicrobial, *Oral Microbes,* ADMET, Drug likeness analysis, *In vitro, In silico*

Introduction

Piper crocatum contains essential oils, alkaloids, flavonoids, tannin-polyphenols, steroids and neolignan compounds [1-3]. In pharmacological studies, Red Betel extract shows a variety of biological activities such as antioxidant, antitumour, anticancer, antidiabetic, antihyperglycemic, antifungal and antibacterial [4,5]. Research on the antibacterial activity of *P. crocatum* essential oil containing myrcene and kamfena which can inhibit the growth of *S. mutans*, besides that it is also known that in *P. crocatum* leaves there is a stigmasterol compound that actively inhibits *S. mutans. S. sanguinis, E. faecalis* and *C. albicans* [6,7]. The potential of *P. crocatum* as an antifungal has also been proven in several studies such as in the research of Singburaudom

et al. [8] obtained information that the ethanol extract of *P. crocatum* leaves at a concentration of 40% v/v has an effective inhibition against the growth of the fungus *C. albicans* ATCC 10231 with the highest inhibition width (13.3 mm). In addition, *P. crocatum* leaves have also successfully isolated alkaloid compounds that are active in inhibiting *C. albicans* ATCC 10231 [9].

Antimicrobial inhibition can be achieved through several pathways, one of which is by inhibiting the central dogma cycle (DNA replication, transcription and translation) [10]. This cycle plays a very important role as a source of functional proteins from DNA, which in turn drives all microbial metabolism and cellular activity so that microbes can survive, reproduce and interact with their environment. One enzyme that plays an important role in the central dogma process is the DNA ligase enzyme, which connects DNA fragments during the replication process (Okazaki fragments) and repairs DNA damage, as well as in genetic recombination, ensuring that broken single strands of DNA can be reconnected into a complete and stable DNA structure [11,12]. Consequently, the inhibition of DNA ligase results in the inhibition and subsequent eradication of microbial organisms. In addition to the inhibition of the central dogma cycle, the inhibition of cell membrane synthesis can also be achieved. For example, the enzyme lanosterol 14α-demethylase functions in the synthesis of essential sterols by converting lanosterol into further products, such as ergosterol in fungi [13,14]. This enzyme represents a primary target for antifungal drugs due to its crucial role in the survival of fungi, as its inhibition has been demonstrated to disrupt the formation of fungal cell membranes.

Arbain *et al*. [2] reported two neolignan compounds from the bicyclo[3.2.1]octanoid guianin group, named (1′R,2′R,3′S,7S,8R)-Δ5′,8′-2′-acetoxy-3,4,5,3′,5′-pentamethoxy-4′-oxo-8.1′,7.3′-neolignan and (1′R,2′R,3′S,7S,8R)-Δ5′,8′-2′-hydroxy-3,4,5,3′, 5′-penta methoxy-4′-oxo - 8.1′,7.3′-neolignan, isolated from the leaves of Indonesian red betel, *Piper crocatum* Ruiz & Pav. Both compounds have been reported to have been tested for several activities such as antibacterial, antileishmanial, anti-inflammatory and xanthine oxidase inhibition assay, but they were not active in all of these activity tests.

Several studies have shown that *P. cocatum* has potential as an antimicrobial agent and can be used in the search for alternative drugs for oral infections. Currently, the search for alternative drugs is very important due to the emergence of microbial resistance to several antibiotics. This study aims to isolate active antimicrobial compounds from red betel leaves and predict their inhibitory mechanisms against DNA ligase and lanosterol 14α demethylase enzymes, so that the compounds obtained can be used as starting compounds in the development of oral infection drugs. In this study, the activity of crocatin A and B compounds, successfully isolated from red betel leaves, against oral pathogenic microorganisms namely, the bacteria *S. mutans*, *S. sanguinis* and *E. faecalis*, as well as the fungus *C. albicans* was reported *in vitro* and *in silico*. Additionally, we also reported the results of ADMET analysis and drug suitability to determine the potential of these two compounds as drug candidates.

Materials and methods

Materials for isolation and *In vitro* antimicrobial activity assay

The material used to isolate the active compound was *Piper crocatum*, sourced from Bekasi, West Java, Indonesia. The extraction, separation and purification of solvents utilised distilled organic solvents, namely methanol, *n*-hexane and ethyl acetate. Analytical grade organic solvents were obtained from Merck Co. Separation by column chromatography (CC) used Silica G 60 (Merck, Darmstadt, Germany) and ODS RP-18, while for Thin Layer Chromatography (TLC) Silica G 60 F_{254} and ODS RP-18 $F_{254}S$ plates (Merck, Darmstadt, Germany) were used. Visualisation of compound spots on TLC was performed under UV light at 254 and 356 nm as well as spraying with 10% H_2SO_4 in EtOH and heating. The antimicrobial test utilised *S. mutans* ATCC 25175, *S. sanguinis* ATCC 10556, *E. faecalis* ATCC 29212 and *Candida albicans* ATCC 10231. The media employed for bacteria were Muller Hinton Agar (MHA) and Muller Hinton Broth (MHB), with the positive control being chlorhexidine. The media used for fungi was Potato Dextrose Agar (PDA), physiological NaCl and Potato Dextrose Broth (PDB). Fluconazole was used as a positive control. Methanol and sterile water as negative control.

Materials for *in silico* molecular docking analysis

The 3D structure of DNA ligase was obtained from the Protein Data Bank (PDB) ID: 1TA8.[15] DNA ligase enzyme from UniProt Knowledgebase (http://www.uniprot.org/): UniProtKBQ837V6. The DNA ligase enzyme generated by the Swiss model using the 1TA8 template showed 100% sequence identity. While the 3D structure of lanosterol 14α-demethylase enzyme was obtained from Protein Data Bank (PDB) ID: 5V5Z [7,16]. Lanosterol 14α-demethylase enzyme from UniProt Knowledgebase (http://www.uniprot.org/): UniProtKBP10613. The lanosterol 14α-demethylase enzyme generated by the Swiss model using template 5V5Z showed 100% sequence identity. The chemical structure of crocatin B and crocatin A was generated using ChemDraw 2D and the minimum energy was calculated using ChemDraw 3D. The positive control in the bacterial inhibition test was chlorhexidine (CID 9552079) and the positive control in the fungal inhibition test was Fluconazole (CID 3365). All data were obtained from PubChem compound database (https://www.ncbi.nlm.nih.gov/pccompound).

Methods

Isolation and antimicrobial activity assay In vitro

The isolation process was guided by antimicrobial bioactivity tests against oral microbes such as *S. mutans, S. anguinis, E. faecalis* and *C. albicans*. Bioactivity testing was carried out starting from the extract and the separation or purification of compounds was carried out using column chromatography with a certain gradient system monitored by thin layer chromatography. Each fraction of the separation results with column chromatography is tested for activity in Kirby Bauer until a pure compound is obtained, then the pure compound obtained is tested for antimicrobial activity again in agar diffusion (Kirby Bauer) and dilution (MIC, MBC or MFC).

In silico assay of DNA ligase and lanosterol 14-α-demethylase enzymes

The crocatin B and crocatin A compounds were drawn using ChemDraw 2D and the three-dimensional structures were converted using ChemDraw 3D format and saved as PDB format. The DNA ligase and lanosterol 14α demethylase enzymes were extracted from the RCSB protein database with PDB IDs 1TA8 and 5V5Z, respectively and saved in PDB format. The *in silico* assay was analysed by the moleculer docking method using Autodock 4.0. The DNA ligase and lanosterol 14α-demethylase enzymes were isolated from their native ligands using the BIOVIA Discovery Studio programme and stored in the PDB format. Subsequently, crocatin B and the positive control were docked to the DNA ligase and lanosterol 14α-demethylase enzymes that had been free from their natural ligands using Autodock 4.0. The receptors and ligands, which had been stored in pdbqt format, were opened in order to set the grid box and docking area. They were then saved in gpf format. Binding of the receptor and ligand was carried out using genetic algorithm parameters, which had been stored in dpf format. Both files were docked on the command prompt using Autogrid4 and Autodock4 formulas. The best conformations were selected based on bond affinity and the lowest Ki value calculated. Subsequently, the interaction of the Mpro enzyme with the three compounds was visualised using the BIOVIA Discovery Studio program.

ADMET and drug-likeness analysis

The absorption, distribution, metabolism and excretion (ADME) of the compound were predicted using the online web servers pkCSM (http://biosig.unimelb.edu.au/pkcsm/) and Swiss ADME (http://www.swissadme.ch/index.php). The toxicity prediction and Lipinski Rule of Five were predicted using the online web server (https://tox-new.charite.de/protox_II/) [17].

Results

Isolation and characterisation of crocatin A and crocatin B

Red Betel leaves with a total mass 5 kg were cut into small pieces and extracted using the maceration method with methanol as the solvent (3×24 h). The cutting of the red betel leaves was conducted with the objective of increasing the surface area of the sample, thereby facilitating greater interaction between the sample and the solvent and enabling optimal extraction conditions [18]. In this study, each stage in compound isolation was guided by bioactivity testing (Bioassay guided). The methanol extract of Red Betel leaf

obtained was tested for antimicrobial activity against *S. mutans, S. sanguinis* and *E. faecalis* bacteria and *C. albicans* fungus. The methanol extract of Red Betel leaves was concentrated until a concentrated extract (30 g) was obtained. The concentrated Red Betel methanol extract was then separated by column chromatography using Silica G 60 stationary phase (0.063 - 0.200 mm). The eluent used was *n*-hexane: Ethyl acetate solvent with a 10% gradient.

The results of the separation by column chromatography obtained fourteen fractions. In testing the antimicrobial activity of the fourteen fractions against bacteria *S. mutans, S. sanguinis, E. faecalis* and fungus *C. albicans*, several fractions were obtained that were active both on all four microbes and were specifically active on certain microbes, one of which was fraction eight. Fraction eight was purified using column chromatography with Silica G 60 RP F_{254}s stationary phase and H_2O: Methanol eluent with a 2.5% gradient starting from a solvent ratio of 3: 2 until twelve fractions were obtained. Pure compounds were obtained from the recrystallization process in fraction five (F 8.5) and obtained compound 1 with a mass of 214 mg with characteristics in the form of colorless needle-shaped solids soluble in methanol, 2D KLT analysis showed a single stain pattern that only glowed under UV light 254 nm and on H_2SO_4 stain sprayer showed a yellow stain pattern.

Isolate compound 1 was characterized by UV-Vis, FTIR, NMR and MS spectrometry. The results of UV-Vis spectrum analysis of compound 1 showed two peaks at wavelengths of 205, 5 and 265.5 nm. The infrared spectra showed typical absorption of -OH group at 3,433 cm^{-1}, C-H sp^2 stretch at 3,078 cm^{-1}, C-H sp^3 stretch at 2,936 and 2,839 cm^{-1}, C=O stretch vibration at 1,687 cm^{-1}, aromatic and aliphatic C=C stretching vibrations at λmaks 1,617 and 1,589 cm^{-1} and C-O stretching vibrations at λmaks 1,238 cm^{-1}, O-CH_3 stretching vibrations at λmaks 1,122 cm^{-1} and alkene C-H bending at λmaks 694 cm^{-1} [19].

The results of ^{1}H-NMR spectrum analysis showed the presence of protons from 5 methoxy groups which appeared at δH 3.28 (3H, *s*), 3.63 (3H, *s*), 3.80 (6H, *s*) and 3.70 (3H, *s*). In addition to protons from methoxy groups, aromatic protons, olefins and protons from methyl groups were also found, each of which appeared at δH H 6.28 (2H, *s*), 6.38 (1H, *s*), 5.90 (1H, *m*) and 1.27 (3H, *d,* 7.0 Hz). The ^{1}H-NMR spectrum of compound 1 showed the presence of several methine sp^3 protons appearing at δH H 2.26 (1H, *m*), 3.35 (1H, *s*) and oxygenated methine sp^3 at 3.94 ppm (1H, *s*). The protons of the allyl group appeared at δH 5.90 (1H, *m*), 5.25 (1H, *dd*), 5.14 (1H, *dd*), 2.75 (1H, *m*) and 2.36 (1H, *m*). ^{13}C-NMR and DEPT 135 spectra of compound 1, known in compound 1 there are 23 carbon atoms consisting of 8 quaternary carbons including sp^3 quaternary carbons at chemical shifts of 49.3 and 96.3 ppm and six sp^2 quaternary carbons at chemical shifts of 134.5; 136.5; 152.0; 152.5 (2x); 194.5 ppm. The DEPT 135 spectrum of compound 1 also showed two negative peaks which were peaks of two methylene carbons at δC 34.2 and 117.5 ppm. There are seven methine carbons suspected consisting of sp^3 methine carbons at δC 48.1 and 59.2 ppm, oxygenated methine carbons that appear at δC 78.6 ppm and four sp^2 methine carbons at δC 134.7, 127.6, 105.9 (2x) ppm. In addition, six methyl carbons are suspected with one carbon appearing at δC 16.1 ppm as sp^3 methyl carbon and the other five methyl carbons appearing as methoxy at δC 53.0; 54.3; 54.9 (2x); and 59.6 ppm. Based on the characterisation results, it is known that compound 1 is a crocatin B compound. This was confirmed through mass spectroscopy analysis (ESI-TQD-MS). Based on the literature, it is known that crocatin B has a molecular weight of 418 g/mol [2]. The results of positive ion spectrum analysis (ES^+) conducted on compound 1 show that compound 1 has a molecular weight of 419 g/mol, so the actual molecular weight value is 418 g/mol. this shows the suitability of the molecular formula $C_{23}H_{30}O_7$ which is a crocatin B compound.

Compound 2 was obtained from fractions 6 and 7, fractions 6 and 7 had the same stain pattern and both were active against *S. sanguinis* so fractions 6 and 7 were combined and purified using ODS RP-18 column chromatography. Pure isolate was obtained at F 6.10 with clear needle-shaped crystal characteristics. Compound 2 can fluoresce in UV light 254 nm and 10% H_2SO_4 stain spotter, but does not fluoresce in UV light 365 nm. Pure compounds with a concentration of 20 ppm show two peaks, namely at a wavelength of 211.5 which comes from the conjugation band (B band) which is aromatic benzene functional groups with electron transitions $\pi \rightarrow \pi^*$ and absorption at a the wavelength of 264.5 nm originates from the radical band (R band) of a

single chromophore group, which possesses a lone pair with electron transitions n → π* [20]. Based on the tests carried out, it is known that compound 2 contains unsaturated ketone groups and acetyl ketones which appear at wave numbers 1,703.1 and 1,748.4 cm^{-1}, aromatics at wave numbers 1,590.4, 1,510.9 and 1,462.8 cm^{-1}. Vinyl groups appearing at a wavelength of 915.4 cm^{-1}. Compound 2 has a structural framework similar to compound 1, only different in its functional groups. Compound 2 does not contain an OH group, the OH group in compound 2 is replaced with an OAc group, so compound 2 is known as crocatin A. The structures of compounds 1 and 2 can be seen in **Figure 1**.

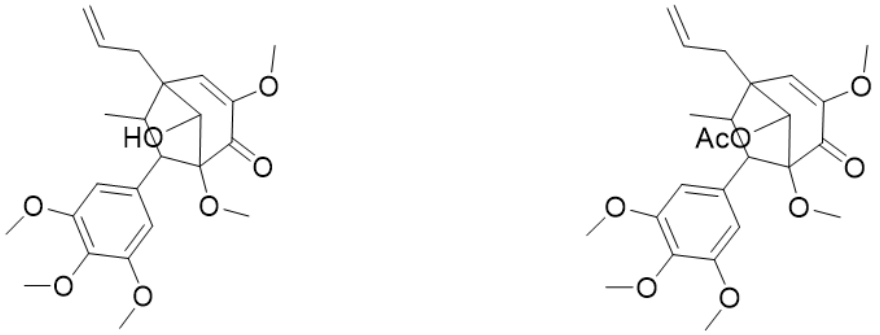

(1) **(2)**

Figure 1 Structure of compounds (**1)** crocatin B and (**2)** crocatin A.

***In vitro* antimicrobial activity of crocatin B and crocatin A**

Antimicrobial activity testing was carried out by agar diffusion method by measuring the diameter of the inhibition zone and by MIC and MBC dilutions. The inhibition zone diameter values of crocatin B against *S. mutans, S. sanguinis* and *E. faecalis* bacteria can be seen in **Figures 2** and **3** for inhibition zone diameter values against *C. alicans*. The values of Minimum Inhibitory Concentration and Minimum Bactericidal Concentration or Minimum Fungicidal Concentration of crocatin B (1) are as shown in Table 1. Based on the literature, the inhibition zone value of crocatin B (1) compound shows moderate antibacterial activity against the three test microbes, which is classified based on the antibacterial strength scale (i.e. > 20 very strong, 10 - 20 strong, 5 - 10 moderate, 2 - 5 weak) [21].

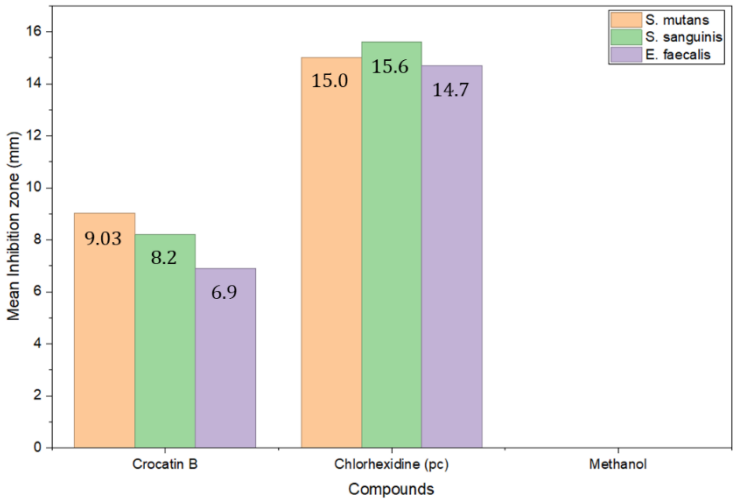

Figure 2 Zone of inhibition of crocatin B, Chlorhexidine (pc) and methanol (nc) at a concentration of 2% against bacteria *S. mutans, S. sanguinis* and *E. faecalis* with.

The antifungal test in **Figure 3** shows that crocatin B (1) compound has moderate activity against *C. albicans* ATCC 10231 at concentrations of 2.5 and 5%. Based on the reference, the inhibition zone is said to be strong if it is more than 6 mm, moderate if it ranges from 3 - 6 mm and weak if it is less than 3 mm [14,22]. This shows the good potential of crocatin B (1) which was successfully isolated from Red Betel leaf

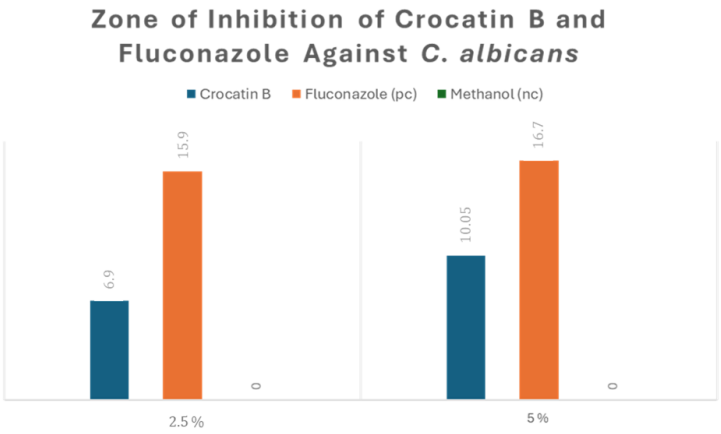

Figure 3 Zone of inhibition (mm) of crocatin B and Fluconazole against *C. albicans*.

MIC and MBC test data in **Table 1** show that crocatin B (1) compounds have MIC values in the moderate range against *S. sanguinis* and *C. albicans*, strong against *S. mutans* and *E. faecalis*, when viewed from the MIC values against the four microbes it can be seen that crocatin B has the most optimal potential in inhibiting *S. mutans*. Based on the reference, the MIC value is referred to as a very strong category if the MIC < 100 µg/mL, strong (101 > MIC ≤ 500 µg/mL) and moderate (501 >MIC < 625 µg/mL), weak 1,000 to 2,000 µg/mL and inactive if the MIC value is > 2,000 [23].

Table 1 MIC, MBC and MFC values of crocatin B (1) and crocatin A (2) compounds.

Compound	*S. mutans*		*S. sanguinis*		*E. faecalis*		*C. albicans*	
	MIC	**MBC**	**MIC**	**MBC**	**MIC**	**MBC**	**MIC**	**MFC**
crocatin B	156.3	3750	937.5	7500	187.5	1,500	781.3	6250

The crocatin A compound was only tested for activity against *S. sanguinis* bacteria, this was because the mass of the crocatin A compound was not as much as the crocatin B (1) compound. The results of the *in vitro* test of crocatin A (**2**) compound produced an MIC value of 2,500 µg/mL, which showed weak inhibitory activity against *S. sanguinis* bacteria.

***In silico* antimicrobial activity of crocatin B and crocatin A**

In silico studies of crocatin B (1) and crocatin A (2) compounds were modelled as inhibitors of one bacterial enzyme, DNA ligase (PDB ID: 1TA8) and one fungal enzyme, lanosterol 14α demethylase (PDB ID: 5V5Z). The results of this *in silico* activity test will obtain values in the form of bond affinity values (ΔG) and inhibition constants (Ki). The inhibitory activity of crocatin B and crocatin A against both target enzymes showed potential results, and when compared the two compounds crocatin A has a higher inhibitory potential than crocatin B based on its more negative binding affinity value. The results of *in silico* tests of crocatin B (1) and crocatin A (2) compounds against the target protein, namely the DNA ligase enzyme can be seen in

Tables 2 and **3** for inhibition data against lanosterol 14-α demethylase enzyme. The molecular interactions of crocatin B (1) and crocatin A (2) can be seen in **Figures 4** and **5**.

Table 2 Binding affinity values and inhibition constants against DNA ligase.

Compounds	Banding Affinity (Kcal/mol)	Inhibition Constant/Ki (μM)
crocatin B	–6.14	36.37
crocatin A	–7.27	4.71
Chlorhexidine (pc *in vitro*)	–12.88	3.61×10^{-4}
Native Ligand	–7.77	2.02

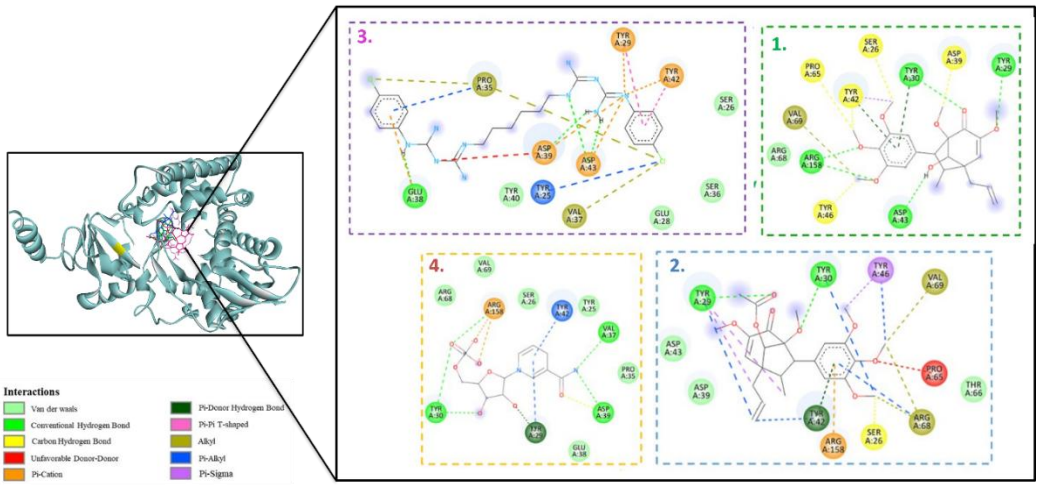

Figure 4 Molecular Interaction of (1) crocatin B, (2) crocatin A, (3) chlorhexidine and (4) native ligand to DNA ligase Enzyme.

Table 3 Binding affinity values and inhibition constants against lanosterol 14-α demethylase.

Compounds	Banding Affinity (Kcal/mol)	Inhibition Constant/Ki (μM)
crocatin B	–7.91	1.58
crocatin A	–9.04	0.236
Fluconazole (pc *in vitro*)	–7.36	4.00
Native Ligand	–6.51	16.95

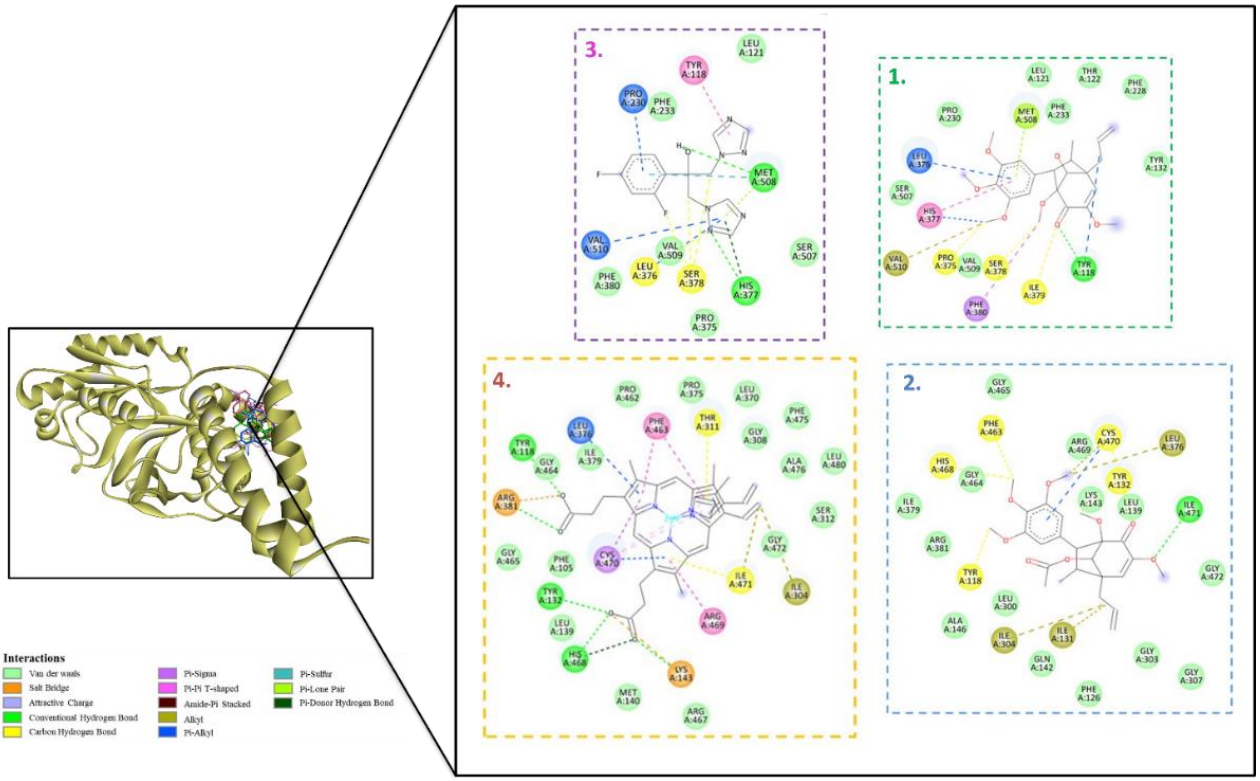

Figure 5 Molecular Interaction of (1) crocatin B, (2) crocatin A, (3) fluconazole and (4) native ligand to lanosterol 14α-demethylase enzyme.

ADMET dan RO5 analysis

ADMET analysis is assessed from several parameters, the first parameter is the absorption parameter of the drug compound including water solubility and drug absorption in the gut, etc. The second parameter is the distribution of the drug compound in the body which can be determined from the volume of distribution (VDss), Blood-Brain Barrier (BBB) permeability, and Central Nervous System (CNS) permeability.[24] The third parameter is the metabolism of the drug compound in the body, the metabolism of the drug can be predicted by determining whether the drug inhibits CYP enzymes. CYP enzymes, also known as Cytochrome P450, are a group of enzymes that play a role in the digestive system and phase 1 metabolic processes.[25] The fourth pharmacokinetic parameter that must be considered is the excretion system, and finally, toxicity, which is categorised into four classes based on lethal dose. The interpretation data of the ADMET analysis results of crocatin B (1) and crocatin A (2) compounds are as shown in **Table 4**. The Swiss ADME analysis results, specifically the boiled egg graph, categorise compounds according to their lipophilicity (WlogP) and topological polar surface area (TPSA) [26,27]. The graph displays two main regions: The yellow region (‘egg yolk’), which indicates a compound’s ability to cross the blood–brain barrier (BBB) and is therefore suitable for central nervous system (CNS) drugs [28,29]. However, drugs that cross the BBB tend to have more side effects. The white region (‘egg white’) indicates good gastrointestinal absorption and is therefore ideal for orally administered drugs with a better safety profile [30]. Compounds in this region are likely to have favourable pharmacokinetic profiles for their respective routes of administration. Compounds outside these two regions may require optimisation to improve their absorption and distribution properties. crocatin A and crocatin B (**Figure 6**) are located in the white region, suggesting that both compounds are expected to have good gastrointestinal absorption and are therefore suitable for oral administration.

Table 4 Interpretation data of the ADMET analysis results of crocatin B (1) and crocatin A (2).

Properties	Parameters		crocatin B	crocatin A
Absorption	Water Solubility		–5.077 log mol/L	–5.665 log mol/L
	Intestinal Absorption		98.266%	100%
Distribution	Volume Distribution (VDss)		0.181 log L/Kg	0.059 log L/Kg
	BBB Permeability		–0.81 log BB	–1.102 log BB
	CNS Permeability		–3.184 log PS	–3.19 log PS
Metabolism	Inhibitor of	CYP1A2	No	No
		CYP2C19	No	No
		CYP2C9	No	No
		CYP2D6	No	No
		CYP3A4	Yes	Yes
Excretion	Total Clearance		0.359 mL/min/kg	0.587 mL/min/kg
Acute Oral Toxicity	Lethal Dose 50%		1050 mg/kg	1050 mg/kg

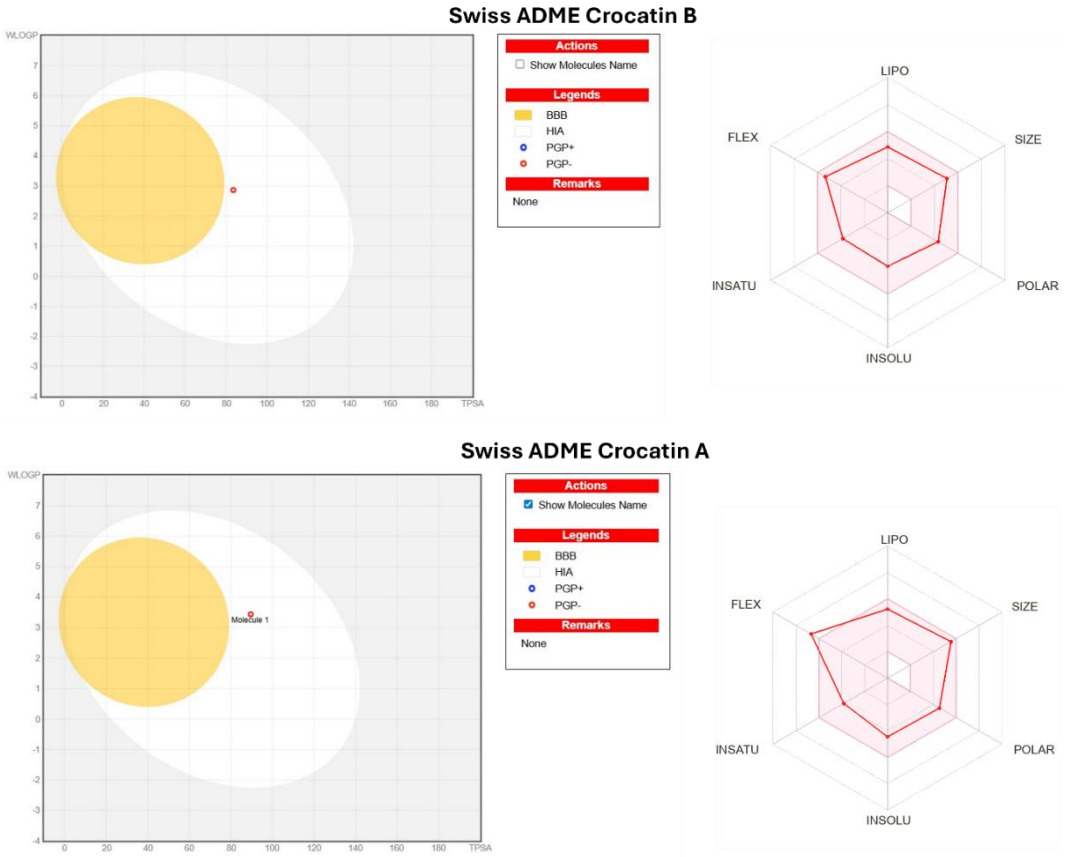

Figure 6 ADME analysis result of crocatin A and crocatin B.

Drug likeness analysis of a compound can be performed according to Lipinski's Rule of Five (RO5). A compound can be evaluated for its chemical and physical properties with a view to determining its suitability for use as an active drug [31]. Compounds crocatin B (1) and crocatin A (2) are predicted to be suitable for use as drugs based on Lipinski's rule, as for the results of drug likeness analysis of crocatin B and crocatin A as contained in **Table 5**.

Table 5 Drug similarity analysis *Lipinski Rule of Five* (RO5) crocatin B (1) and crocatin A (2).

Parameters	crocatin B	crocatin A
Molecular mass (< 500 Dalton)	418	460.52
Hydrogen bond donor (< 5)	1	0
Hydrogen bond acceptors (< 10)	7	8
LogP (< 5)	2.87	3.44
Molar Refractivity (40 - 130)	111.51	121.25
Violation	0	0
Drug-likeness	Yes	Yes

Discussion

Two-dimensional nuclear magnetic resonance characterisation of components 1 and 2

Two-dimensional NMR analyses include ^{1}H-^{1}H COSY, HMBC and NOESY analyses. The results of H-H COSY spectrum analysis showed the correlation of H3 (2.23 ppm, 1H, *m*) with H1 (1.24 ppm, 3H, *d*, 7.0 Hz) and H9 (3.34 ppm, 1H, *d*, 6.4 Hz), as well as the correlation between H2 (2, 71 ppm, 2H, *dd*, 7.5 & 13.8 Hz) with H18 (5.25 & 5.14 ppm, 2H, *dd*, 1.75 & 17.2 Hz) and H18 (5.90 ppm, 1H, *m*), in addition it was also found to have a correlation to H15. The next two-dimensional NMR analysis is HMBC (**Figure 7**), through HMBC analysis it can be seen the correlation of protons to carbon with a distance of 3 - 4 bonds. Based on HMBC analysis, it can be seen that some specific proton and carbon correlations such as the correlation of H1 (1.27 ppm, *d*, *J* = 7.0 Hz) to C3 (48.1 ppm) and C9 (59.2 ppm). Further correlations between H2 to C4 (49.3 ppm), C15 (117.5 ppm), C16 (127.6 pmm) and C18 (134.7 ppm) [2], as well as correlations of protons to carbon 3 - 4 other bonds as can be seen in **Figure 4**. In the NOESY spectrum of crocatin B (1) compound, it can be seen that there are several proton correlations in the molecular space of crocatin B (1) compound, and several correlations are obtained, namely between H11 (1H, s, 3.94 ppm) to H16 (1H, s, 6.38 ppm), H1 (1.24 ppm, 3H, *d*, 7.0 Hz) with H3 (2.23 ppm, 1H, *m*), H2 (2.71 ppm, 2H, *dd*, 7.5 & 13.8 Hz), H16 (1H, *s*, 6.38 ppm) and several other NOESY correlations as shown in **Table 6**.

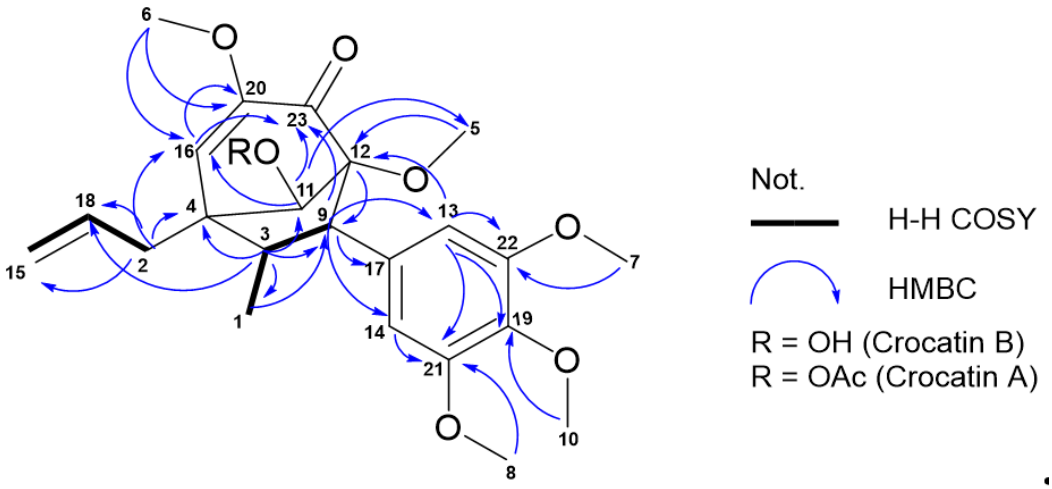

Figure 7 Structure and ^{1}H-^{1}H COSY and HMBC correlations of crocatin B (1) and crocatin A (2).

Table 6 Interpretation of data from NMR analyses of crocatin B (**1**).

No.	δ_C (ppm)	δ_H (ppm)	^{1}H-^{1}H COSY	HMBC	^{1}H-^{1}H NOESY
1	16.1	1.27	H1 → H3	H1 → C3; C9	H1 → H2, H3 H1 → H17 H1 → H13, H14 H1 → H16
2	34.2	2.36;2.75	H2 → H18	H2 → C4; C11, C15, C16, C18, C20	H2 → H11 H2 → H15 H2 → H16
3	48.1	2.26	H3 → H1	H3 → C1; C4; C9; C11; C16; C18	H3 → H13, H14
4	49.3	-	-	-	-
5	53.0	3.28	-	H5 → C12	-
6	54.3	3.63	-	H6 → C16, C20	H6 → 16
7	54.9	3.80	-	H7 → C8	H7 → H13, H14
8	54.9	3.80	-	H8 → C14; C21	H8 → H13, H14
9	59.2	3.35	H9 → H3	H9 → C1; C3; C12; C13; C17; C23	-
10	59.6	3.70	-	H10 - C19	-
11	78.6	3.94	-	H11 → C5; C9; C16; C23	H11 → H16
12	96.3	-	-	-	-
13	105.9	6.28	-	H13 → C12; C19; C21; C22	-

No.	δ_C (ppm)	δ_H (ppm)	^{1}H-^{1}H COSY	HMBC	^{1}H-^{1}H NOESY
14	105.9	6.28	-	H14 → C12; C19; C21; C22	-
15	117.5	5.14;5.25	H15 → H18	H15 → C2; C18	H15 → H16 H15 → H17
16	127.6	6.38		H16 → C3; C2; C12; C20; C23	-
17	134.5	-	-	-	H17 → H16
18	134.7	5.90	-	H18 → C2	-
19	136.5	-	-	-	-
20	152.0	-	-	-	-
21	152.5	-	-	-	-
22	152.5	-	-	-	-
23	194.5	-	-	-	-

Biogenesis crocatin B (1) and crocatin A (2)

Molecular docking analysis

The docking process was carried out by validating the method on the receptor by redocking between the native ligand to the receptor, redocking to DNA ligase was carried out at coordinates x = 6.062, y = 32.743, z = 26.151 (40×40×40) while redocking to lanosterol receptor 14α demethylase was carried out at coordinates x = –44.744, y = –9.025, z = 23.391 (40×40×40). Based on *in silico* results, namely affinity data and inhibition constants, it can be seen that the inhibitor of DNA ligase binding affinity of crocatin A (2) is better than crocatin B (1), which is –7.27 Kcal/mol, but it cannot outperform the binding affinity of the native ligand and positive control used in *in vitro* studies. This can occur due to several factors, one of which is due to the interaction of compounds with amino acid residues of the target protein, for example hydrogen, hydrophobic or electrostatic interactions. Based on the results of docking four ligands to the DNA ligase enzyme, it is known that chlorhexidine has the best binding affinity of –12.88 Kcal/mol and a Ki value of 3.61×10^{-4}. The binding affinity value indicates the stability of the conformation formed when the ligand binds to the macromolecule, with stability ranked from best to worst, from the lowest to the highest value. The Ki value indicates the inhibition constant of the ligand compound against the receptor. The smaller the Ki value, the lower the inhibition constant, which means that the ligand compound has the potential to inhibit the receptor better [36]. When viewed from the type of interaction that occurs between chlorhexidine and the amino acid residues involved (**Figure 4**), there are several interactions, including 3 amino acid residues that form hydrogen bonds with chlorhexidine, namely GLU A:38, ASP A:39 and ASP A:43. Four amino acid residues were also found to interact electrostatically, namely SER A:26, SER A:36, GLU A:26 and TYR A:40.

In addition, seven amino acid residues were also found to form hydrophobic interactions, including VAL A:37, TYR A:25, ASP A:43, ASP A:39, TYR A:42, TYR A:29 and PRO A:35. Furthermore, when viewed from the original substrate of the DNA ligase enzyme, DNA as a whole is acidic (negatively charged) and binds to a basic protein (positively charged) called histone [37]. This suggests that potential inhibition of the DNA ligase enzyme will be optimal if the ligand contains a charge opposite to the active site or has properties similar to DNA, which contains positively and negatively charged parts. In the docking results of the

native ligand and chlorhexidine, there are pi-cation and pi-anion interactions. These interactions involve attractive forces between ionic charges and pi electron clouds in aromatic systems, resulting in good binding affinity. Similarly, crocatin A has pi-cation interactions, which may be one of the reasons for its better binding affinity compared to crocatin B (1). Similarly, inhibition of the lanosterol 14α demethylase enzyme by the four test ligands showed that crocatin A had the best binding affinity value of –9.04 kcal/mol and a Ki value of 0.236, which was even better than the original ligand. This occurs because the hydrogen interaction between crocatin A (2) and the amino acid residue of the lanosterol 14α demethylase enzyme is the most abundant among the three other test ligands. The types of interactions that occur between crocatin B (1), crocatin A (2), the original ligand and chlorhexidine against DNA ligase can be seen in **Table 7**. **Table 8** shows the types of interactions between crocatin B (1), crocatin A (2), the original ligand and fluconazole against the lanosterol 14α demethylase enzyme.

Table 7 The type of interaction that occurs between crocatin B (1), crocatin A (2), native ligand and chlorhexidine against DNA ligase.

Category	Type of interaction	Compounds against DNA ligase Enzyme			
		Native ligand	**Chlorhexidine**	**crocatin B**	**crocatin A**
Hydrogen bond	Conventional	ASP A:39, VAL A:37, TYR A:30	GLU A: 38, ASP A:39, ASP A:43	TYR A:30, TYR A:29, ASP A:43, ARG A: 158	TYR A:30, TYR A:29
Carbon-hydrogen bond		ASP A:39	-	SER A:26, ASP A:39, TYR A:42, PRO A:65, TYR A: 46	SER A:26
Hydrophobic	Pi-Alkyl	TYR A:42	TYR A:25, PRO A:35	-	TYR A:46, TYR A: 30, TYR A:42, TYR A:29, ARG A:68
	Pi-Pi -stacked	-	TYR A:29, TYR A:42	-	-
	Pi-sigma	-	-	-	TYR A:46
	Alkyl	-	PRO A:35, VAL A:37	VAL A:69	VAL A:69, ARG A:68
	Pi- Donor Hidrogen	TYR A:29	-	TYR A:42, TYR A:30	TYR A:42
	Pi- sulfur	-	-	-	-
	Pi- lone pair	-	-		-
Unfavorable	Donor-Donor	-	ASP A:39	ARG A:68	-

Category	Type of interaction	Compounds against DNA ligase Enzyme			
		Native ligand	**Chlorhexidine**	**crocatin B**	**crocatin A**
Electrostatic	Acceptor-Acceptor	-	-	-	PRO A:65
	Attractive charge	ARG A:158	ASP A:39, ASP A:43	-	-
	Pi-cation	-	TYR A:29, TYR A:42	-	ARG A:158
	Pi-anion	-	GLU A:38	-	-
	Van der Waals	GLU A:38, PRO A:35, TYR A:25, SER A:26, VAL A:69, ARG A:68	SER A:26, GLU A:28, SER A:36, TYR A:40	ARG A:68	THR A:66, ASP A:39, ASP A:43

Table 8 The type of interaction between crocatin B (1), crocatin A (2), native ligand and Fluconazole against lanosterol 14α-demethylase.

Category	Type of interaction	Compounds against Lanosterol 14α-demethylase Enzyme			
		Native ligand	**Fluconazole**	**crocatin B**	**crocatin A**
Hydrogen bond	Conventional	TYR A: 132, HIS A:468, TYR A:118	HIS A:377, MET A:508	TYR A: 118	ILE A:471
Carbon-hydrogen bond		-	LEU A:376, SER A:378	ILE A:379, SER A:378, PRO A:375	CYS A:470, TYR A:132, PHE A:463, HIS A:468, TYR A:118
Hydrophobic	Pi-Alkyl	LEU A:376	PRO A:230, LEU A:376, VAL A:510	LEU A:376	CYS A:470
	Pi-Pi -stacked	PHE A:463	TYR A:118	HIS A:377	-
	Pi-sigma	CYS A:470	-	PHE A:380	-
	Alkyl	ILE A:304, ILE A:471	-	VAL A:510	LEU A:376, ILE A:131, ILE A:304
	Pi- Donor Hidrogen	THR A:311, ILE A:471	-	-	-
	Pi- sulfur	-	MET A:508	-	-

Category	Type of interaction	Compounds against Lanosterol 14α-demethylase Enzyme			
		Native ligand	**Fluconazole**	**crocatin B**	**crocatin A**
	Pi- lone pair	-	MET A:508	MET A:508	-
	Attractive charge	ARG A:381 LYS A:143	-	-	-
	Halogen	-	SER A:378	-	-
Unfavorable	Donor-Donor	-	HIS A:375	-	-
	Acceptor-Acceptor	-	-	-	-
Electrostatic	Van der Waals	ARG A:467, MET A:140, LEU A:139, GLY A:465, PHE A:105, GLY A:464, ILE A:379, PRO A:462, PRO A:375, LEU A:370, GLY A:308, PHE A:475, ALA A:476, LEU A:480, SER A:312, GLY 472	LEU A:121, PHE A:233, PRO A:375, PHE A:380, SER A:507, VAL A:509	SER A:507, VAL A:509, TYR A:132, PHE A:238, THR A:122, PHE A:233, LEU A:121, PRO A:230	GLY A:465, ARG A:469, LYS A:143, LEU A:139, GLY A:472, GLY A:303, GLY A:307, PHE A:126, GLN A:142, LEU A:300, ALA A:146, ARG A:381, ILE A:379, GLY A:464

ADMET and drug-likeness analysis

Computational modelling studies can be employed to investigate drug pharmacokinetics, encompassing the observation and analysis of absorption, distribution, metabolism, excretion and toxicity (ADMET). The advantage of predicting the pharmacokinetics of a compound through computational studies is that this method can reduce costs and enhance efficiency. Bioactive compounds that have been isolated from plants can be regarded as superior compounds if they exhibit a favourable ADMET profile.

In terms of absorption parameters, it is essential to consider both water solubility and intestinal absorption. Water solubility is a crucial factor in the bioavailability of a drug. Water solubility is categorised as optimal if the water solubility value is within the range of less than 0 and greater than –0.5 [38,39]. In this study, the water solubility of crocatin B (1) and crocatin A (2) compounds was within the predetermined range of –5.077 and –5.665 log mol/L. In contrast, for absorption in the intestine, a drug compound is included in the good category if the absorption value in the intestine is above 80% [40] crocatin B (1) and crocatin A (2) has an intestinal absorption value of 99.03 and 100%, indicating that the crocatin B (1) and crocatin A (2) compounds can be absorbed well in the intestine.

The distribution of drugs or lead compounds in the body is analysed using three parameters: Volume of distribution, blood-brain barrier (BBB) permeability and central nervous system (CNS) permeability [24]. The volume of distribution of a drug or compound is typically within the range of 0.5 to 3 L/kg. crocatin B (1) and crocatin A (2) have a relatively effective drug delivery system in the blood. A drug is classified as

effective if it is challenging to penetrate the central nervous system (CNS) or even difficult to reach the blood-brain barrier (BBB). The absorption value of a drug into the CNS and BBB is categorised into three groups: High absorption (value > 2.0), moderate absorption (value between 0.1 - 2.0) and low absorption (value < 0.1) [24]. Absorption values of 0 and less than 0.1 are indicative of low absorption, while values greater than 0.1 are indicative of high absorption [41]. The crocatin A (2) compound has an absorption value of less than 0.1, thus falling within the low absorption category and crocatin B (1) has an moderate absorption. This indicates that the crocatin B (1) and crocatin A (2) compounds are challenging to penetrate the central nervous system (CNS) and blood-brain barrier (BBB).

The metabolism of a drug can be predicted by determining whether the drug inhibits CYP enzymes. CYP enzymes, also known as Cytochrome P450, are a group of enzymes that play a role in the digestive system and phase 1 metabolic processes [25]. These three test compounds had no inhibition of these various types of CYP enzymes. crocatin B (1) and crocatin A (2) only inhibits one type of CYP enzyme, namely CYP3A4. The final pharmacokinetic parameter that must be considered is the excretion system. The faster the excretion process of a molecule, the higher the total clearance value [17]. There is evidence that this has a positive effect on the body. The total clearance value of crocatin B (1) and crocatin A (**2**) (0.359 and 0.587 mL/min/Kg) indicates that the compounds have a fairly good excretion process.

Toxicological prediction science can be carried out using computational techniques as an effort to reduce the necessity for toxicity testing on experimental animals. In testing with computational techniques, the results obtained are also similar to those obtained from *in vivo* tests. The toxicity level ratio is seen from the Lethal Dose value [42,43]. The lethal dose 50 (LD_{50}) is a parameter that determines whether a compound is toxic or not [44]. The LD_{50} criteria are divided into six classes, class 1 which is a group of drugs or drug substances considered fatal if ingested when the LD_{50} value is less than 5 mg/kg. Class II with values between $5 < LD_{50} \leq 50$ mg/kg is classified as fatal if swallowed. Class III group of drugs or drug substances with a value of $50 < LD_{50} \leq 300$ mg/kg with an indication of poison if swallowed. Class IV for drugs or drug substances with a value of $300 < LD_{50} \leq 2{,}000$ mg/kg which are classified as dangerous if swallowed. Class V is a group of drugs or drug substances that may be harmful if swallowed with a value of $2{,}000 < LD_{50} \leq 5{,}000$ mg/kg. Class VI drugs or drug substances are classified as non-toxic if the LD_{50} is greater than 5,000 mg/kg [24]. The compound from this study, crocatin B (1) and crocatin A (2) are categorised as dangerous if swallowed. Consequently, it can be used as a medicine or a mixture of mouthwash to prevent oral infections caused by pathogenic oral microbes.

Drug-likeness analysis of a compound can be conducted in accordance with the Lipinski Rule of Five (RO5). A compound can be evaluated for its chemical and physical properties with a view to determining its suitability for use as an active drug [31]. Lipinski RO5 conforms to the following rules: Molecular mass less than 500 Daltons, number of hydrogen bond acceptors < 5, number of hydrogen bond donors less than 10, molar refractivity value 40 - 130 and Log P value less than 5. **Table 7** shows that crocatin B (1) and crocatin A (2) show no violation of the RO5 rule. Furthermore, the rule stipulates that a compounds may be employed as a drug orally if it does not exhibit more than one violation [45]. Furthermore, in the event that a compound exhibits two or more violations of Rule of Five (RO5), its solubility and permeability are significantly diminished.

Conclusions

Based on the data obtained, crocatin B (1) and crocatin A (2) are compounds that have potential as antimicrobials against oral pathogenic microbes as evidenced by *in vitro* and *in silico* studies. From the pharmacokinetic (ADME) and drug likeness parameters crocatin B (1) and crocatin A (2) compounds also show good results, but the oral toxicity of both compounds is included in class 4 so it is more recommended to be used as a constituent in mouthwash (not swallowed) to overcome oral infection problems or can be used as the main compound for further research and treatment.

Acknowledgements

The authors are grateful to Universitas Padjadjaran for all research facilities. This study was funded by Lembaga Penelitian dan Pengabdian kepada Masyarakat (LPPM) No. 001/LPPM-UP/KPFR/VI/2025.

Declaration of Generative AI in Scientific Writing

The authors emphasize that generative artificial intelligence tools (such as QuillBot, DeepL, and ChatGPT from OpenAI) were used exclusively for language refinement and grammar correction during the preparation of this manuscript. These tools were not used to generate content or interpret data. The authors are solely responsible for the content and conclusions of this work.

CRediT Author Statement

Leny Heliawati: Supervision, data analysis, validation, and editing draft. **Seftiana Lestari:** Draft preparation, Data curation, Investigation, Data analysis, and Editing draft. **Yusrina Imani:** Data curation, Investigation, and Data analysis. **Tri Aminingsih:** Data validation, editing draft. **Asri Wulandari:** Data validation, editing draft. **Dikdik Kurnia:** Supervision, conceptualization, Validation, and Writingreview & editing.

Reference

[1] N Parfati and T Windono. Red betel (*Piper crocatum* Ruiz & Pav) literature review. *Media Pharmaceutica Indonesiana* 2016; **1(2)**, 106-115.

[2] D Arbain, Nofrizal, N Syafni, F Ismed, S Yousuf and MI Choudhary. Bicyclo[3.2.1]octanoid neolignans from Indonesian red betle leaves (*Piper crocatum* Ruiz & Pav.). *Phytochemistry Letters* 2017; **24**, 163-166.

[3] YJ Chai YJ Chai, Y Go, HQ Zhou, HX Li, SJ Lee, YJ Park, W Widowatib, R Rizal, YH Kim, SY Yang and W Li. Unusual bicyclo[3.2.1]octanoid neolignans from leaves of *Piper crocatum* and their effect on pyruvate dehydrogenase activity. *Plants* 2021; **10(9)**, 1855.

[4] FO Enwa. Mechanisms of antimicrobial actions of phytochemicals against enteric pathogens - A Review. *Journal of Pharmaceutical Biological and Chemical Sciences* 2014; **2(2)**, 77-85.

[5] Emrizal, A Fernando, R Yuliandari, K Rullah, NR Indrayani, A Susanty, R Yerti, F Ahmad, HM Sirat and D Arbain. Cytotoxic activities of fractions and two isolated compounds from Sirih Merah (Indonesian red betel), *Piper crocatum* Ruiz & Pav. *Procedia Chemistry* 2014; **13**, 79-84.

[6] D Kurnia, S Lestari, T Mayanti, M Gartika and D Nurdin. Anti-infection of oral microorganisms from herbal medicine of *Piper crocatum* Ruiz & Pav. *Drug Design, Development and Therapy* 2024; **18**, 2531-2553.

[7] S Lestari, D Kurnia, T Mayanti and L Heliawati. Antimicrobial activities of stigmasterol from *Piper crocatum in vitro* and *in Silico*. *Journal of Chemistry* 2024; **2024(1)**, 2935516.

[8] N Singburaudom. Hydroxychavicol from *Piper betel* leave is an antifungal activity against plant pathogenic fungi. *Journal of Biopesticides* 2015; **8(2)**, 82-92.

[9] T Siswina, MM Rustama, D Sumiarsa, E Apriyanti, H Dohi and D Kurnia. Antifungal constituents of *Piper crocatum* and their activities study using ADMET and drug-likeness Analysis. *Molecules* 2023; **28(23)**, 7705.

[10] E Eijk, B Wittekoek, EJ Kuijper and WK Smits. DNA replication proteins as potential targets for antimicrobials in drug-resistant bacterial pathogens. *The Journal of Antimicrobial Chemotherapy* 2017; **72(5)**, 1275-1284.

[11] K Bilotti, V Potapov, JM Pryor, AT Duckworth, JL Keck and GJS Lohman. Mismatch discrimination and sequence bias during end-joining by DNA ligases. *Nucleic Acids Research* 2022; **50(8)**, 4647-4658.

[12] KP Ha and AM Edwards. DNA Repair in *Staphylococcus aureus*. *Microbiology and Molecular Biology Reviews: MMBR* 2021; **85(4)**, e0009121.

[13] WD Nes, M Chaudhuri and DJ Leaver. Druggable sterol metabolizing enzymes in infectious diseases: Cell targets to therapeutic leads. *Biomolecules* 2024; **14(3)**, 249.

[14] T Siswina, MM Rustama, D Sumiarsa and D Kurnia. Phytochemical profiling of *Piper crocatum* and its antifungal activity as Lanosterol 14 alpha demethylase CYP51 inhibitor: A review. *F1000Research* 2023; **11**, 1115.

[15] KS Gajiwala and C Pinko. Structural rearrangement accompanying NAD+synthesis within a bacterial DNA ligase crystal. *Structure* 2004; **12(8)**, 1449-1459.

[16] MV Keniya, M Sabherwal, RK Wilson, MA Woods, AA Sagatova, JDA Tyndall and BC Monk. Crystal structures of full-length lanosterol

14α-Demethylases of prominent fungal pathogens candida albicans and candida glabrata provide tools for antifungal discovery. *Antimicrobial Agents and Chemotherapy* 2018; **62(11)**, e01134-18.

[17] D Kurnia, SA Putri, SG Tumilaar, A Zainuddin, HDA Dharsono and MF Amin. *In silico* study of antiviral activity of polyphenol compounds from *Ocimum basilicum* by molecular docking, ADMET and drug-likeness analysis. *Advances and Applications in Bioinformatics and Chemistry : AABC* 2023; **16**, 37-47.

[18] NV Wendersteyt, DS Wewengkang and SS Abdullah. Uji aktivitas antimikroba dari ekstrak dan fraksi ascidian herdmania momus dari perairan pulau bangka likupang terhadap pertumbuhan mikroba *Staphylococcus aureus*, *Salmonella typhimurium* dan *Candida albicans*. *Pharmacon* 2021; **10(1)**, 706-712.

[19] MF Yahaya, JM Yelwa, S Abdullahi, JB Umar, AM Abubakar and M Babakura. Chemical compositions, FTIR and larvicidal activity of essential oils extracted from aromatic plants. *European Scientific Journal* 2019; **15(24)**, 110.

[20] KC Lin, B Muthiah, HP Chang, T Kasai and YP Chang. Halogen-related photodissociation in atmosphere: Characterisation of atomic halogen, molecular halogen and hydrogen halide. *International Reviews in Physical Chemistry* 2020; **40(1)**, 1-50.

[21] TI Purwantiningsih, W Haumein and J Presson. Air rebusan daun sirih sebagai antibakteri alami untuk mencegah mastitis. *Jurnal Ilmu dan Teknologi Peternakan Tropis* 2020; **7(3)**, 252.

[22] AS Ravipati, N Reddy and SR Koyyalamudi. *Biologically active compounds from the genus Uncaria (Rubiaceae)*. *Studies in Natural Products Chemistry* 2014; **43**, 381-408.

[23] CM Mouzié, MGF Guefack, BY Kianfé, HU Serondo, BK Ponou, X Siwe-Noundou, RB Teponno, RWM Krause, V Kuete and LA Tapondjou. A new chalcone and antimicrobial chemical constituents of dracaena stedneuri. *Pharmaceuticals* 2022; **15(6)**, 725.

[24] J Leszczynski, A Kaczmarek-Kedziera, T Puzyn, MG Papadopoulos, H Reis and MK Shukla. *Handbook of computational chemistry*. Springer, Cham, Switzerland.

[25] Y Guttman and Z Kerem. Computer-aided (*In Silico*) modeling of cytochrome P450-Mediated food-drug interactions (FDI). *International Journal of Molecular Sciences* 2022; **23(15)**, 8498.

[26] F İslamoğlu and E Hacıfazlıoğlu. Investigation of the usability of some triazole derivative compounds as drug active ingredients by ADME and molecular docking properties. *Moroccan Journal of Chemistry* 2022; **10(4)**, 861-880.

[27] M Jeleń, B Morak-Młodawska, M Dołowy and A Konefał. Study of the Lipophilicity of Tetracyclic Anticancer Azaphenothiazines. *Biomolecules* 2025; **15(8)**, 1194.

[28] N Pavlović, NM Sopta, D Mitrović, D Zaklan, AT Petrović, N Stilinović and S Vukmirović. Principal component analysis (PCA) of molecular descriptors for improving permeation through the Blood–Brain barrier of quercetin analogues. *International Journal of Molecular Sciences* 2024; **25(1)**, 192.

[29] D Mitrović and N Pavlović. *In silico* approach in the development of structural analogues of resveratrol with improved distribution in the central nervous system. *Kragujevac Journal of Science* 2024; **46(1)**, 59-71.

[30] H Sardar. Drug like potential of Daidzein using SwissADME prediction: *In silico* approaches. *PHYTONutrients* 2023; **2(1)**, 02-08.

[31] CA Lipinski. Lead- and drug-like compounds: The rule-of-five revolution. *Drug Discovery Today: Technologies* 2004; **1(4)**, 337-341.

[32] F Cotinguiba, HM Debonsi, RV Silva, RM Pioli, RA Pinto, LG Felippe, SN López, MJ Kato and M Furlan. Amino acids L-phenylalanine and L-lysine involvement in trans and cis piperamides biosynthesis in two Piper species. *Brazilian Journal of Biology* 2023; **82**, e268505.

[33] JE Poulton and VS Butt. Purification and properties of S-adenosyl-l-methionine: Caffeic acid o-methyltransferase from leaves of spinach Beet (Beta vulgaris L.). *Biochimica et Biophysica Acta (BBA) – Enzymology* 1975; **403(2)**, 301-314.

[34] JM Humphreys, MR Hemm and C Chapple. New routes for lignin biosynthesis defined by biochemical characterization of recombinant

ferulate 5-hydroxylase, a multifunctional cytochrome P450-dependent monooxygenase. *Proceedings of the National Academy of Sciences of the United States of America* 1999; **96(18)**, 10045-10050.

[35] C Paniagua, A Bilkova, P Jackson, S Dabravolski, W Riber, V Didi, J Houser, N Gigli-Bisceglia, M Wimmerova, E Budínská, T Hamann and J Hejatko. Dirigent proteins in plants: Modulating cell wall metabolism during abiotic and biotic stress exposure. *Journal of Experimental Botany* 2017; **68(13)**, 3287-3301.

[36] HMA El-Lateef, MM Khalaf, M Kandeel, AA Amer, AA Abdelhamid and A Abdou. Designing, characterization, biological, DFT and molecular docking analysis for new FeAZD, NiAZD and CuAZD complexes incorporating 1-(2-hydroxyphenylazo)−2-naphthol (H2AZD). *Computational Biology and Chemistry* 2023; **105**, 107908.

[37] S Sato, M Dacher and H Kurumizaka. Nucleosome structures built from highly divergent histones: Parasites and giant DNA viruses. *Epigenomes* 2022; **6(3)**, 22.

[38] P Augustijns, B Wuyts, B Hens, P Annaert, J Butler and J Brouwers. A review of drug solubility in human intestinal fluids: Implications for the prediction of oral absorption. *European Journal of Pharmaceutical Sciences* 2014; **57**, 322-332.

[39] G Falcón-Cano, C Molina and MÁ Cabrera-Pérez. ADME prediction with KNIME: *In silico* aqueous solubility consensus model based on supervised recursive random forest approaches. *ADMET & DMPK* 2020; **8(3)**, 251-273.

[40] MF Khan, N Nahar, RB Rashid, A Chowdhury and MA Rashid. Computational investigations of physicochemical, pharmacokinetic, toxicological properties and molecular docking of betulinic acid, a constituent of Corypha taliera (Roxb.) with Phospholipase A2 (PLA2). *BMC Complementary and Alternative Medicine* 2018; **18(1)**, 48.

[41] XL Ma, C Chen and J Yang. Predictive model of blood-brain barrier penetration of organic compounds. *Acta Pharmacologica Sinica* 2005; **26(4)**, 500-512.

[42] VM Alves, EN Muratov, A Zakharov, NN Muratov, CH Andrade and A Tropsha. Chemical toxicity prediction for major classes of industrial chemicals: Is it possible to develop universal models covering cosmetics, drugs and pesticides. *Food and Chemical Toxicology* 2018; **112**, 526-534.

[43] AA Toropov, AP Toropova, I Raska, D Leszczynska and J Leszczynski. Comprehension of drug toxicity: Software and databases. *Computers in Biology and Medicine* 2014; **45(1)**, 20-25.

[44] MN Drwal, P Banerjee, M Dunkel, MR Wettig and R Preissner. ProTox: A web server for the *in silico* prediction of rodent oral toxicity. *Nucleic Acids Research* 2014; **42(W1)**, W53-W58.

[45] LZ Benet, CM Hosey, O Ursu and TI Oprea. BDDCS, the Rule of 5 and drugability. *Advanced Drug Delivery Reviews* 2016; **101**, 89-98.